Chemical Science & Engineering Research

Ariviyal Publishing

Research Article

DOI:10.36686/Ariviyal.CSER.2023.05.12.067

Chem. Sci. Eng. Res., 2023, 5(12), 1-7.

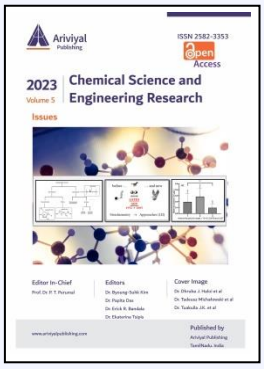

Physico-Chemical Characterization of Agro-Waste Sugarcane Bagasse Ash from Three Brazilian Sugarcane Mills and Obtaining Biosilica from Ash

Rovani S.,[a] Santos J.J.,[b] Carvalho F.B.,[a] Ramos N.P.,[c] Saldanha M.,[c] Morandi M.A.B.[c] and Fungaro D.A.*[a]

[a]*Instituto de Pesquisas Energéticas e Nucleares (IPEN-CNEN/SP) - Av. Prof. Lineu Prestes, 2242, Cidade Universitária, 05508-000, São Paulo, SP.*

[b]*Instituto de Química, Universidade de São Paulo - Av. Prof. Lineu Prestes, 748, Cidade Universitária, Box 26077, 05508-000, São Paulo, SP.*

[c]*Embrapa Meio Ambiente. Rod. SP 340, km 127, 5. Caixa Postal 69 Jaguariúna, SP.*

***Corresponding author E-mail address**: dfungaro@ipen.br (Fungaro D. A.)

ISSN: 2582-3353

Crossref

Publication details
Received: 21st November 2022
Revised: 10th March 2023
Accepted: 10th March 2023
Published: 29th March 2023

Abstract: The interest in transforming biomass into new sources of energy and new materials has been encouraging studies around the world. The ash resulting from the burning of straw and sugarcane bagasse, for example, is a material rich in silica. In the present study, samples of fly ash and bottom ash from sugarcane residues were collected in three different mills (Cerradinho Iracema and Guaíra), located in regions where the soils are classified as oxisols. The ashes were characterized by XRD, EDX, ICP-OES, SEM, FTIR spectroscopy and TGA/DTG techniques. Most ash samples showed silica as the main constituent (42-69%) and silica in crystalline form in all. Biosilica was obtained from ash samples using alkali extraction and acid precipitation. The physical and chemical properties of the extracted biosilica are described. The biosilica samples have amorphous phases and purity ranged from 93 to 97 wt.%. The results showed that the different origins of sugarcane residue ash used as raw material did not affect the quality of the extracted biosilica.

Keywords: sugarcane bagasse; biomass waste; agricultural residue ash; biosilica; sustainability

1. Introduction

Brazil is the largest producer of sugarcane in the world, followed by India, China, Thailand, Pakistan and Mexico. According to CONAB, Brazil produced a total of 642.7 million tons of sugarcane in the 2019/2020 harvest.[1]

Sugarcane bagasse ash (SCBA) is the by-product generated on large scale as a result of the burning of sugarcane bagasse in energy cogeneration. There about 2.5% of the mass from the cane is transformed into ash, of which most of its reuse is in the form of fertilizers in Brazil and China[2] and is generally disposed of in landfills in others countries.[3]

The use of SCBA as fertilizers mixed with vinasse can alter the physical and chemical characteristics of soil.[4] In addition, SCBA has a low nutritional value and heavy metals may penetrate into the ground and pollute the soil and groundwater.[2]

Thus, studies that evaluate others possibilities of reusing the SCBA in addition to use as a fertilizer are promising, given that this material will have a destination in an ecological and economical way.[5]

Ashes from sugarcane residues can be considered suitable renewable raw material for obtaining biosilica because present SiO_2 as the main chemical compound. The conditions under which the bagasse is burned in the boiler (600–800°C) for electricity generation produces ash with polymorphic and amorphous crystalline phases. Synthesis of silica from agrowaste materials has become a considerable concern because of its physicochemical properties and wide industrial application.[6-8]

The physical properties and compositions of SCBA vary with many factors, such as sugarcane varieties, combustion temperature and duration, purity of bagasse, bagasse ash collection, cooling type, boiler equipment, ash fineness, etc.[9] Bagasse ash collected from the bottom of the boiler is coarser and contain irregular particles, and the bagasse ash collected through a filtration system contains less carbon and finer particles.[10] It was estimated that 11% of the ashes generated in boilers are fly ash-type, whereas 89% of the ashes are bottom-type.[11]

The main aim of this study is to investigate the physicochemical characteristics of bottom and fly bagasse ash generated by three different sugarcane mills. The characteristics of biosilica derived from these residues as a possible alternative source for reuse was also investigated.

Table 1. Chemical composition of sugarcane waste ash samples

	(wt. %)				
	C-BA[1]	I-1A-FA[2]	I-1B-BA[3]	G-2A-FA[4]	G-2B-BA[5]
SiO_2	68.88	54.96	65.26	42.10	25.37
Fe_2O_3	13.80	12.64	14.24	33.61	59.99
CaO	8.092	9.361	5.929	3.713	1.603
K_2O	5.835	11.19	8.718	6.839	3.286
TiO_2	2.483	4.439	3.168	7.889	3.936
P_2O_5	-	4.032	-	-	-
SO_3	-	2.358	1.227	0.900	1.752
BaO	0.572	-	0.874	3.131	2.930
V_2O_5	-	-	-	0.606	-
MnO	0.197	0.506	0.353	0.587	0.329
ZrO_2	-	0.155	-	0.153	0.124
ZnO	0.096	0.088	0.034	0.060	0.074
SrO	0.044	0.076	0.053	0.051	-
CuO	-	0.082	-	-	0.107
Cr_2O_3	-	0.077	0.119	0.014	0.490

(1) Cerradinho-Bottom Ash; (2) Iracema 1A –Fly Ash; (3) Iracema 1B-Bottom Ash; (4) Guaíra 2A-Fly Ash; (5) Guaíra 2B-Bottom Ash

Table 2. Trace elements content of the sugarcane waste ash samples

	(mg kg^{-1})				
	C-BA[1]	I-1A-FA[2]	I-1B-BA[3]	G- 2A-FA[4]	G-2B[5]
Ca	5829	9202.9	2831.4	9556.8	769.9
Mg	2146	4940.6	1863.2	4284.1	350.3
Na	530	-	-	-	-
K	7534	13657.9	4609.4	17206.2	5592.0
Al	16896	17166.1	3893.2	27390.7	24109.6
Cu	11	29.5	7.2	68.2	120.1
Fe	14595	9255	16621	22162	43751
Mn	135	437.6	236.5	707.1	398.2
Zn	60	50.4	17.8	52.9	52.8
B	10	< D.L.	< D.L.	< D.L.	< D.L.
S	546	983.9	480.8	871.5	147.9
Pb	3	5.0	4.8	2.8	19.2
Cd	< D.L.	< D.L.	< D.L.	< D.L.	< D.L.
Ni	2	4.4	5.9	10.8	18.5
Cr	50	-	-	-	-

(1) Cerradinho-Bottom Ash; (2) Iracema 1A –Fly Ash; (3) Iracema 1B-Bottom Ash; (4) Guaíra 2A-Fly Ash; (5) Guaíra 2B-Bottom Ash (< D.L. = less than the detection limit).

2. Experimental Section

2.1. Materials

All aqueous solutions were prepared using deionized water (resistivity > 18.2 MΩ cm) obtained from a Milli-Q deionizer (Elix Millipore). Five samples of sugarcane ash were collected from two points in the sugarcane mills, three samples were collected at the bottom of the boilers (Cerradinho, Iracema 1A, and Guaíra 2A) and two were collected near the chimney, derived of the washing of gases and particulates with the water (Iracema 1B and Guaíra 2B). The location of the plants is Cerradinho (Chapadão do Céu, Goias, Brazil), Iracema (Iracemápolis, São Paulo, Brazil) and Guaíra (Guaíra, São Paulo, Brazil). Sodium hydroxide micro-pearls (>99%), hydrochloric acid (35-37%) were purchased from Synth, Brazil.

2.2. Synthesis of Biosilica from the Sugarcane Waste Ash

It was first prepared a sodium silicate solution from sugarcane waste ash according to adapted methodology described previously.[12] Briefly, a mixture of ash and sodium hydroxide (proportion of ash : NaOH 1:2.0 w/w) was heated at 350°C for 30 min. Then 100 mL of distilled water was added to the mixture and refluxed for 1 h, and the mixture was filtered to separate the silicate solution from the residue. In the second step, hydrochloric acid solution (6 mol L^{-1}) was slowly added to the sodium silicate solution for complete silica precipitation until the pH decreased to 2.0. The resulting gel was aged at room temperature for 12 h, washed with distilled water, filtered and oven dried at 120°C overnight.

2.3. Characterization Methods

The chemical composition of the samples was analyzed by Energy-dispersive X-ray spectroscopy (EDX), using Shimadzu equipment, and model EDX 720 and by Inductively Coupled Plasma Optical Emission Spectrometry (ICP-OES) model Perkin Elmer Optima 8300. The ash morphology was evaluated by scanning electron microscopy (SEM) using a Hitachi bench microscope, model TM 3000. Before the SEM analysis, the sample was fixed in a sample holder with carbon tape and covered with gold using a sputtering equipment BAL-TEC SAMPLE COATER/SPUTTER, model SCD 050.

The mineralogical analysis of the both samples was performed by X-ray powder diffraction (XRD), using a Rigaku Multiflex diffractometer with Cu anode using Co Kα radiation at 40 kV and 20 mA. The angular velocity was 1° min^{-1} and the scanning interval was 2θ = 5-80°, with a scanning time of 0.5° min^{-1}.

The ashes and the silica were also characterized by Fourier-transform infrared spectroscopy (FTIR) using a Bruker spectrophotometer, model Alpha, operating in the attenuated total reflectance (ATR) mode. The spectrum was obtained using 200 cumulative scans, within the spectral range from 375 to 4000 cm^{-1}.

Thermogravimetric analyzes of the sugarcane waste ash samples were recorded on a TGA/SDTA 851 thermogravimetric analyzer produced by 130 Mettler Toledo. The dry samples (~10.0 mg) were analyzed under an oxygen atmosphere with a flow of 50 mL min^{-1}, using an alumina sample holder heated from room temperature to 900 °C with a heating rate of 10 °C min^{-1}.

Thermogravimetric analyzes of the silica samples were recorded on a DTG-60 (simultaneous DTA-TG apparatus) thermogravimetric analyzer produced by Shimadzu. The dry samples (~5.0 mg) were analyzed under an air atmosphere with a flow of 50 mL min^{-1}, using an alumina sample holder heated from room temperature to 900 °C with a heating rate of 10°C min^{-1}.

3. Results and Discussions

3.1. Characterization of Sugarcane Waste Ash Samples

The chemical composition of each ash of sugarcane residues from the mills was performed by Energy-dispersive X-ray spectroscopy (EDX) and the results are shown in Table 1. The composition of most of the samples is similar and is dominated by SiO_2.The ash from the Cerradinho and Iracema 1B mills presented the highest SiO_2 content among the studied sugarcane waste ash. The SiO_2 content in the ashes of these two mills was similar to published studies by Usina da Barra, Barra Bonita, SP,[2] Usina Sapucaia, Campos dos Goytacazes, RJ[4] and Usina São João da Barra, RJ.[14]

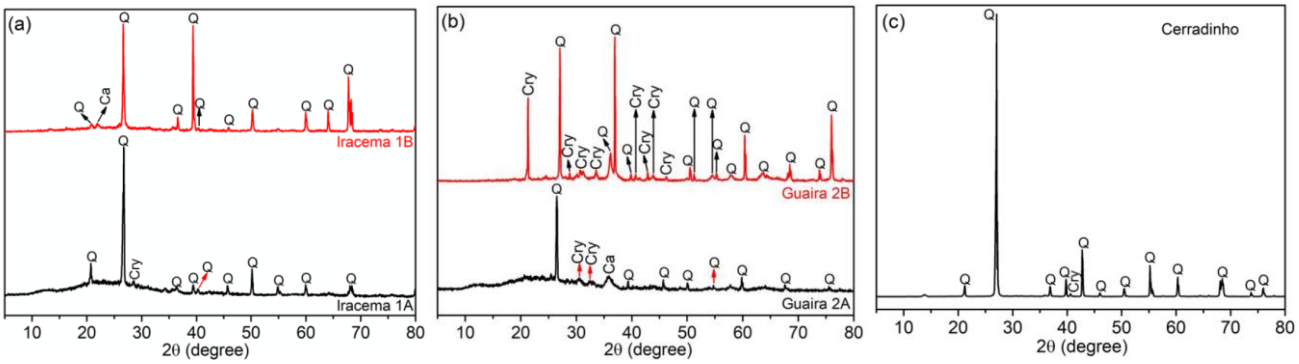

Fig. 1. X-ray diffractograms of the sugarcane waste ash from the mills (a) Iracema 1A (fly ash) - 1B (bottom ash), (b) Guaíra 2A (fly ash) - 2B (bottom ash) and (c) Cerradinho (bottom ash). Q = Quartz; Cry = Cristobalite; Ca = Calcite.

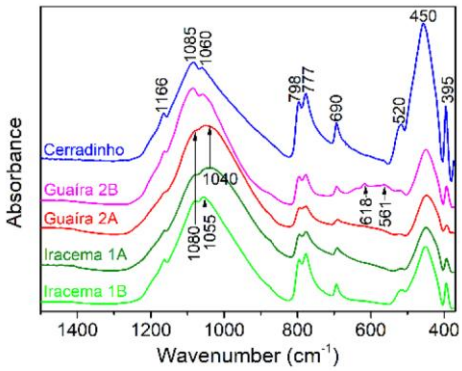

Fig. 2. FTIR-ATR spectra of sugarcane waste ash (fly ash 1A and 2A), (bottom ash 1B, 2B and Cerradinho) from the Iracema, Guaíra and Cerradinho mills.

The type of soil (Brazilian Oxisols) in the sugarcane plantation region can explain the great similarity in the composition. The samples from the Guaíra mill had a different composition from the others, mainly concerning Fe_2O_3 and CaO (high Fe content and low Ca amount), suggesting changes in the original soil (addition of soil acidity correctives, for example). It can be noted that the Guaíra 2B sample presented iron oxide as the main compound.

Semi-quantitative analysis of oxides present in sugarcane ash samples from mills in different regions of the country are in previous studies.[2,4,14-17] The trace elements present in the sugarcane ash samples were determined by ICP-OES (Table 2). The highest concentrations found were for Al, Fe, K, Ca and Mg, which are the same elements observed in residues (straw and bagasse) reported in the literature.[18]

The ash from the Cerradinho and Iracema 1B mills showed the lowest concentrations of most elements, corroborating with the semi-quantitative analysis of the oxides present in the ashes (Table 1).

The X-ray diffractograms of the ash samples from the mills are shown in Fig. 1. In the diffractograms, the presence of only crystalline phases related to quartz, cristobalite, and calcite was observed. The presence of only crystalline phases in these ashes is related to the temperature and burning time of the straw and sugarcane bagasse.

Generally, when the firing temperature is higher than 800°C and a long incineration durations occurs, the amorphous silica present in the sugarcane residues is converted into crystalline silica.[15,19,20]

In addition, the crystalline silica may also come from the sand in the soil, which adheres to the sugarcane.[21] Another result that confirms that the ashes from the Iracema 1B and Cerradinho mills have predominantly crystalline SiO_2 (quartz) can be seen in the X-ray diffractograms in Fig. 1.

The infrared spectra of sugarcane waste ash samples were recorded in the range of 4000-375 cm^{-1}, but the most significant absorption bands were observed only in the range of 1300-375 cm^{-1} (Fig. 2).

The Si-O bonds are the strongest in the silicate structure and can be readily recognized in the infrared spectrum of sugarcane ash. The bands at 1085 or 1080 and 1166 cm^{-1} correspond to the transverse optics (TO) and longitudinal optics (LO) of asymmetric stretching vibrations of the Si-O-Si connection.

The doublet in the 767-816 cm^{-1} range indicates the presence of α-quartz.[22,23] The presence of quartz can also be seen by the asymmetric and symmetrical Si-O angular deformation in 520 and 690 cm^{-1}, respectively.[24-28] The bands at 618 and 561 cm^{-1}, for the sample Guaíra 2 A, is related to double ring vibrations.

The bands at 798 and 450 cm^{-1} are attributed to the symmetrical stretch Si-O-Si.[27,29-31] The band observed at 395 cm^{-1} is related to Si-O-M angular deformation "M = metallic impurities".[24] The band at 1166 cm^{-1} is attributed to the C-C stretch.[32]

The TG and DTG curves of the ash samples were performed under an oxygen atmosphere and are shown in Fig. 3. According to the TG and DTG curves, the greatest mass loss observed in each of the graphs (200-490°C) it is due to the decomposition of organic structures[29] and above 490 °C due to the structural rearrangement that begins with the heating of mineral quartz.[33] Finally, above 600°C, only inorganic components remain.

According to Fig. 3, the ashes from the Iracema 1A and Guaíra 2A mills, both fly ashes, had about 20% carbon and/or organic components. Whereas, the ashes Iracema 1B, Guaíra 2B, and Cerradinho, both bottom ash, presented less than 2 % of carbon and/or organic components. The ashes of the Guaíra 2B mill, despite having a low carbon content and/or organic component, have a very high content of some contaminants such as Al, Fe and have a low Si content (Table 1 and Table 2).

The morphology of the sugarcane waste ash samples supplied by the mills was obtained by scanning electron microscopy (SEM) at different magnifications and is shown in Fig. 3.

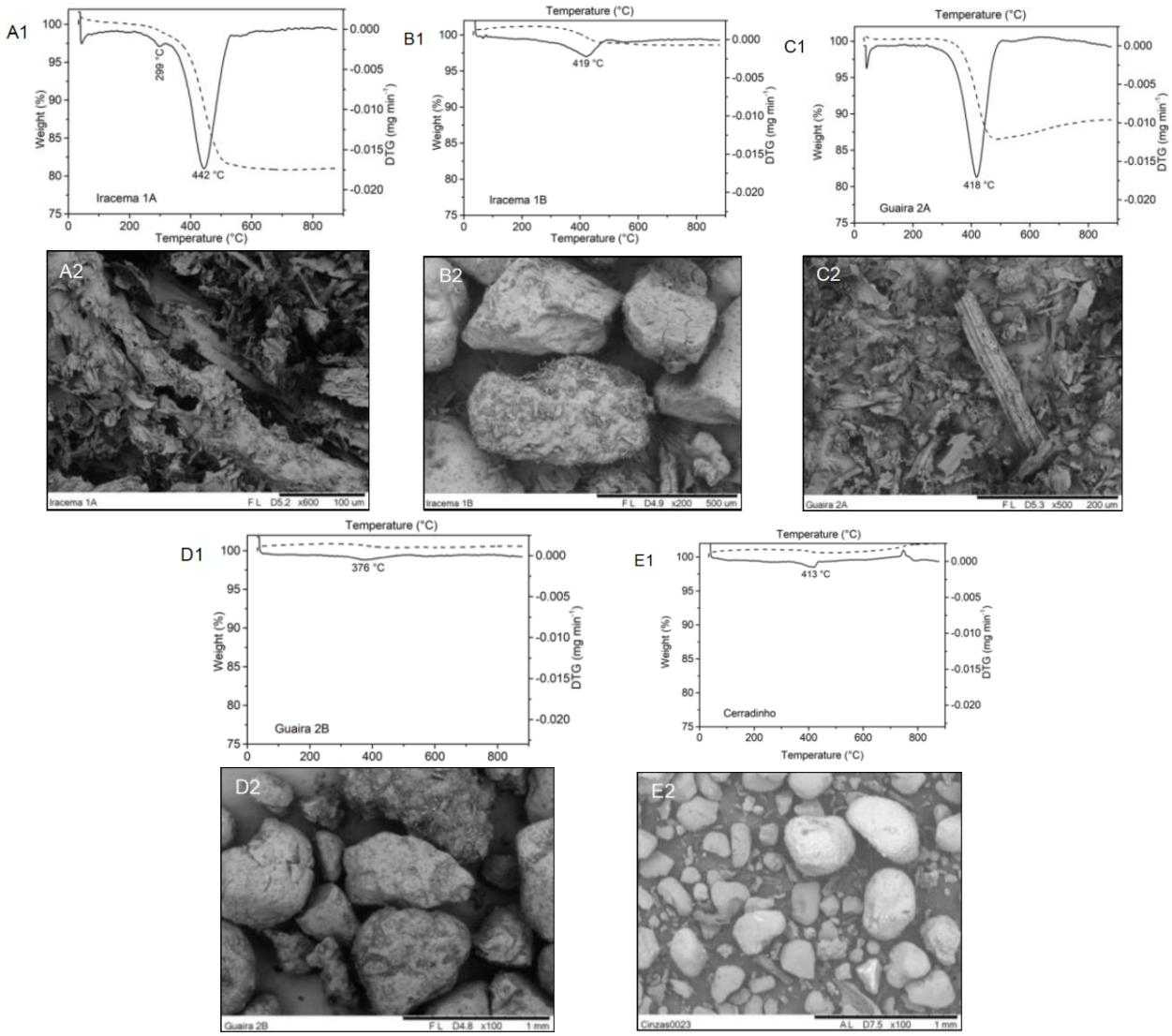

Fig. 3. TG and DTG curves and SEM images of the sugarcane waste ash from the sugarcane mills: Iracema 1A (A1 and A2), Iracema 1B (B1 and B2), Guaíra 2A (C1 and C2), Guaíra 2B (D1 and D2) and Cerradinho (E1 and E2).

The images indicated that the ash particles are quite heterogeneous; the fly ash (A2 and C2) has more fibrous particles.

On the other hand, bottom ash (B2, D2 and E2), that is, boiler bottom ashes, have smooth, round-shaped particles that are characteristic of quartz.[4,15] Some porous particles were also observed. The morphologies of the bottom ash samples are similar to those observed in the literature.[15,34-35]

According to Fig. 3, it was possible to relate the result of TG analyze very well with the SEM images.

The TG curves of the samples A1 and C1 show a great loss of mass weight around 400°C related to the loss of carbon and organic components, and their respective SEM images (A2 and C2) present a fibrous structure characteristic of organic matter.

On the other hand, in the TG curves of the lower ash samples B1, D1 and E1, the loss of mass was minimal and their respective SEM images (B2, D2 and E2) presented larger and rounded particles characteristics of quartz and absence of fibrous material.

Therefore, it can be concluded that in future studies only one of these characterizations already defines whether the material is fly ash or bottom ash.

3.2. Characterization of Silica samples

The experimental procedure used for silica particle synthesis was based on previous studies, where the parameters of the processes have been already optimized.[12] The EDX results indicate that this

Table 3. Chemical composition of silica obtained from sugarcane waste ash of the mills

	(wt. %)				
	Silica[1]	**Silica[2]**	**Silica[3]**	**Silica[4]**	**Silica[5]**
SiO_2	96.19	96.26	96.20	97.10	92.65
Fe_2O_3	1.619	0.939	0.673	0.154	0.717
CaO	-	-	0.017	-	-
K_2O	0.152	0.117	0.190	0.064	0.040
TiO_2	0.264	0.396	0.546	0.150	0.162
SO_3	1.748	2.266	2.226	2.532	1.855
BaO	-	-	0.127	-	-
V_2O_5	0.005	-	-	-	0.090
MnO	0.015	0.010	0.009	-	-
ZrO_2	-	0.002	-	-	-
ZnO	0.010	0.005	-	-	-
Cr_2O_3	-	-	0.014	-	0.007

Silica from:(1) Cerradinho-Bottom Ash; (2) Iracema 1A –Fly Ash; (3) Iracema 1B Bottom Ash; (4) Guaíra 2A-Fly Ash; (5) Guaíra 2B-Bottom Ash

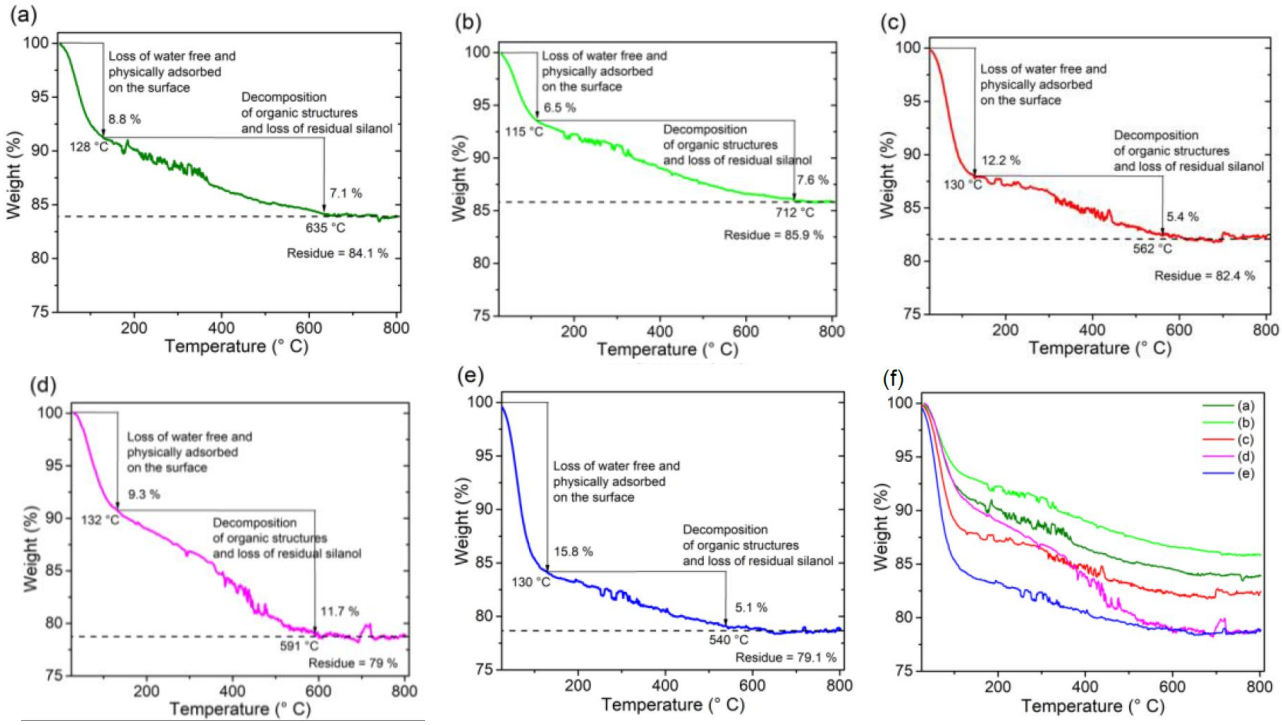

Fig. 4. TG curves of the amorphous silica obtained from the sugarcane waste ash from the mills: (a) Iracema 1A, (b) Iracema 1B, (c) Guaíra 2A, (d) Guaíra 2B, (e) Cerradinho and (f) all TG curves.

Table 4. Thermogravimetric analyses of silica samples

Sample	1° wt. loss (%)	2° wt. loss (%)	Residue (%)
Silica[1]	25 - 130 °C	130 - 540 °C	↑ 540 °C
	15.8	5.1	79.1
Silica[2]	25 - 128 °C	128 - 635 °C	↑ 635 °C
	8.8	7.1	84.1
Silica[3]	25 - 115 °C	115 - 712 °C	↑ 712 °C
	6.5	7.6	85.9
Silica[4]	25 - 130 °C	130 - 562 °C	↑ 562 °C
	12.2	5.4	82.4
Silica[5]	25 - 132 °C	132 - 591 °C	↑ 591 °C
	9.3	11.7	79

Silica from: (1) Cerradinho-Bottom Ash; (2) Iracema 1A –Fly Ash; (3) Iracema 1B-Bottom Ash; (4) Guaíra 2A-Fly Ash; (5) Guaíra 2B-Bottom Ash

silica synthesis method was completely effective for all raw materials (Table 3). From Table 3, confirms that silica (SiO_2) is the predominant compound in all samples. Even in the sugarcane residue ash sample where SiO_2 is not the main element (Guaíra 2B), it was possible to synthesize silica with high purity (93%).

The results of thermal gravimetric analysis (TG) of silica samples are shown in Fig. 4. As reported in the literature, two-step weight losses were observed.

The loss in weight up to 130°C (step 1) is ascribed to dehydration caused by the loss of physically adsorbed H_2O. The second mass loss, between ~130-700°C, can be assigned to the decomposition of remaining organic structures. Above 700°C, no further weight loss was observed indicating thermal stability of extracted silica.[12,36]
The weight loss for each sample is shown in Table 4.

The FTIR spectra for silica samples are shown in Fig. 5. The doublet that indicates the presence of α-quartz in the sugarcane ash samples and the bands in 520 and 690 cm^{-1} referring to quartz, did not appear in the FTIR-ATR spectra of the silica samples.

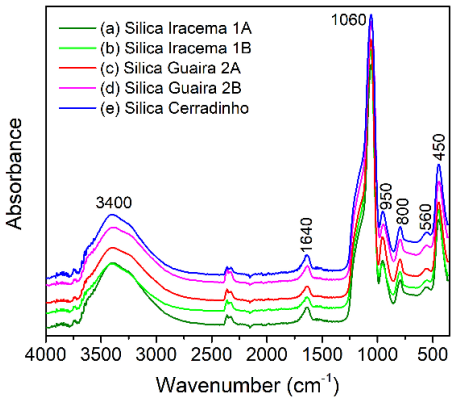

Fig. 5. FTIR-ATR spectra of amorphous silica obtained from the sugarcane waste ash from the mills: Iracema 1A (fly ash) - 1B (bottom ash), Guaíra 2A (fly ash) - 2B (bottom ash) and Cerradinho (bottom ash).

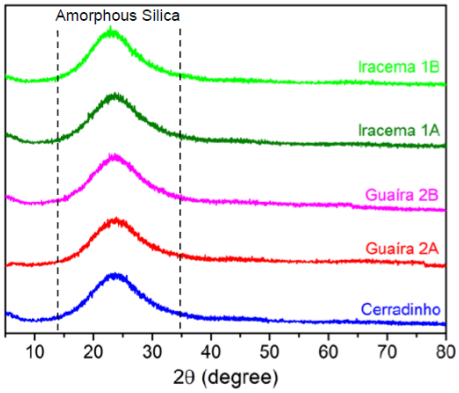

Fig. 6. X-ray diffractograms of the amorphous silica from the sugarcane waste ash of the mills: Iracema 1A (fly ash) - 1B (bottom ash), Guaíra 2A (fly ash) - 2B (bottom ash) and Cerradinho (bottom ash).

This was an indication that the silica samples are amorphous. All the samples showed major peaks at 3400, 1640, 1060, 950, 800, 560 and 450 cm^{-1} which is very close to match with SiO_2 prepared using tetraethylorthosilicate as a silica precursor.[37,38]

The strong band at 1060 cm^{-1} is assigned to Si−O−Si asymmetric stretching, and the band at 950 cm^{-1} is due to the OH angular deformation of free silanol groups. The bands at 800 and 450 cm^{-1} are attributed to the symmetrical stretch Si-O-Si.

In addition, the two bands at 3400 cm^{-1} and 1640 cm^{-1} indicate high-water content with weak interaction in the amorphous silica particles, i.e. the presence of free water. The 560 cm^{-1} band is related to double ring vibrations.[39,40]

The band at 1640 cm^{-1} also corresponds to silica "overtones", silanol forming a bridge or interacting with other species adsorbed on the surface in wavenumbers close to 3400 cm^{-1} which in general produces broad bands. These results agree with the TG analysis of the silica, which indicates high free water content.

Fig. 6 shows the XRD diffractograms of the silica samples from the sugarcane waste ash of the mills. The diffractograms of silica samples indicate the presence of amorphous silica only, which is characterized by the presence of a single broad peak, reaching its maximum around 23° (2θ), corroborating with the literature.[12,16,41]

4. Conclusions

The fly and bottom ash samples collected in three different sugarcane mills (Cerradinho, Iracema and Guaíra) from Sao Paulo State were characterized and four samples present quartz as the main crystalline phase. The ashes generated at the Guaíra mill differed because they contain high concentrations of iron and aluminum and the lowest concentration of silicon oxide among all samples. The vibrational, mineralogical, thermal stability and morphological properties were very similar in the ash samples.

All ash samples could be used as a precursor of biosilica. Precipitated biosilica materials were produced by neutralization of sodium silicate solution with hydrochloric acid solution and presented high purity (93-97% wt% silica content). XRD analysis revealed the appearance of a typical hump indicative of amorphous structure, as FT-IR spectrum and TGA/DTG curves. Considering the continuous generation of sugarcane residue in Brazil, sugarcane waste ash collected in different mills have the potential to be the feedstock for the production of biosilica with good quality.

Acknowledgements

The authors would like to thanks CerradinhoBio (Chapadão do Céu, GO), Usina Iracema of the company São Martinho (Iracemápolis, SP) and Usina Guaíra (Guaíra, SP). This research was funded by the Coordenação de Aperfeiçoamento de Pessoal de Nível Superior-Brasil - Brazil (CAPES) - Financial Code 001.

Conflicts of Interest

The authors declare no conflict of interest.

References

1 CONAB - Companhia Nacional de Abastecimento. 2020. Acompanhamento da safra brasileira de cana-de-açúcar, safra 2019/20, quarto levantamento.
2 Sales A.; Lima S. A. Use of Brazilian Sugarcane Bagasse Ash in Concrete as Sand Replacement. *Waste Manage.*, **30**, 2010, 1114-1122. [CrossRef]
3 Deepika S.; Anand G.; Bahurudeen A.; Santhanam M. Construction Products with Sugarcane Bagasse Ash Binder. *J. Mater. Civ. Eng.*, 2017, **29**, 04017189. [CrossRef]
4 Faria K. C. P.; Gurgel R. F.; Holanda J. N. F. Recycling of Sugarcane Bagasse Ash Waste in the Production of Clay Bricks. *J. Environ. Manage.*, 2012, **101**, 7-12. [CrossRef]
5 Patel H. Environmental Valorisation of Bagasse Fly Ash: A Review. *RSC Adv.*, 2020, **10,** 31611-31621. [CrossRef]
6 Iwuozor K. O.; Ogunfowora L. A.; Oyekunle I. P. Review on Sugarcane-Mediated Nanoparticle Synthesis: A Green Approach. *Sugar Tech*, 2021, **23**, 1186-1197. [CrossRef]
7 Sarkar J.; Mridha D.; Sarkar J.; Orasugh J. T.; Gangopadhyay B.; Chattopadhyay D.; Roychowdhury T.; Acharya Kr. Synthesis of Nanosilica from Agricultural Wastes and its Multifaceted Applications: A Review. *Biocatal. Agric. Biotechnol.*, 2021, **37**, 102175. [CrossRef]
8 Singh J.; Boddula R.; Jirimali H. D. Utilization of Secondary Agricultural Products for the Preparation of Value Added Silica Materials and their Important Applications: A Review. *J. Sol-Gel Sci. Technol.*, 2020, **96**, 15–33. [CrossRef]
9 Katare V. D.; Madurwar M. V. Experimental Characterization of Sugarcane Biomass Ash—A Review. *Constr. Build. Mater.*, 2017, **152**, 1–15. [CrossRef]
10 Molin Filho R.G.D.; Colpini L.M.S.; Ferrer M.M.; Nagano M.F.; Rosso J.M.; Volnistem E.A.; Paraíso P.R.; de Matos Jorge L.M. Characterization of Different Sugarcane Bagasse Ashes Generated for Preparation and Application as Green Products in Civil Construction. *Clean Technol. Environ. Policy*, 2019, **21**, 1687-1698. [CrossRef]
11 Hojo L. Y. C. P. Análise da Atividade Pozolânica da Cinza Volante do Bagaço de Cana-de-Açúcar Para Substituição Parcial do Cimento Portland, State University of Maringá, Maringá, Brazil, 2014, Dissertation.
12 Rovani S.; Santos J. J.; Corio P.; Fungaro D. A. An Alternative and Simple Method for the Preparation of Bare Silica Nanoparticles Using Sugarcane Waste Ash, an Abundant and Despised Residue in the Brazilian Industry. *J. Braz. Chem. Soc.*, 2019, **30**, 1524–1533. [Link]
13 Pérez-Villarejo L.; Eliche-Quesada D.; Iglesias-Godino F.J.; Martínez-García C.; Corpas-Iglesias F.A. Recycling of Ash from Biomass Incinerator in Clay Matrix to Produce Ceramic Bricks. *J. Environ. Manag.*, 2012, **95**, S349-S354. [CrossRef]
14 Cordeiro G. C.; Filho R. D. T.; Fairbairn E. M. R. Caracterização de cinza do bagaço de cana-de-açúcar para emprego como pozolana em materiais cimentícios. *Quim. Nova*, 2009, **32**, **1**, 82-86. [Link]
15 Cordeiro G. C.; Filho R. D. T.; Tavares L. M.; Fairbairn E. M. R. Ultrafine Grinding of Sugar Cane Bagasse Ash for Application as Pozzolanic Admixture in Concrete. *Cem. Concr. Res.*, 2009, **39**, 110-115. [Link]
16 Alves R. H.; Reis T. V. S.; Rovani S.; Fungaro D. A. Green Synthesis and Characterization of Biosilica Produced from Sugarcane Waste Ash. *J. Chem.*, 2017, **2017**, 1-9. [CrossRef]
17 Rodríguez-Díaz J. M.; García J. O. P.; Sánchez L. R. B.; Silva M. G. C.; Silva V. L.; Arteaga-Pérez L. E. Comprehensive Characterization of Sugarcane Bagasse Ash for Its Use as an Adsorbent. *Bioenerg. Res.*, 2015, **8**, 1885–1895. [CrossRef]
18 Formann S.; Hahn A.; Janke L.; Stinner W.; Sträuber H.; Logroño W.; Nikolausz M. Beyond Sugar and Ethanol Production: Value Generation Opportunities Through Sugarcane Residues. *Front. Energy Res.*, 2020, **8**, 579577. [CrossRef]
19 Le Blond J. S.; Horwell C. J.; Williamson B. J.; Oppenheimer C. Generation of Crystalline Silica from Sugarcane Burning. *J. Environ. Monit.*, 2010, **12**, 1459-1470. [CrossRef]
20 Morales E. V.; Villar-Cocina E.; Frias M.; Santos S. F.; Savastano H. Effects of Calcining Conditions on the Microstructure of Sugar Cane Waste Ashes (SCWA): Influence in the Pozzolanic Activation. *Cem. Concr. Compos.*, 2009, **31**, 22–28. [CrossRef]

21 Xu Q.; Ji T.; Gao S. J.; Yang Z.; Wu N. Characteristics and Applications of Sugar Cane Bagasse Ash Waste in Cementitious Materials. *Materials (Basel)*, 2018, **12**, 39-58. [CrossRef]
22 Saoud K. M.; Saeed S.; Bertino M. F.; White L. S. Fabrication of Strong and Ultra-Lightweight Silica-Based Aerogel Materials with Tailored Properties. *J. Porous Mater.*, 2017, 25, **2**, 511-520. [CrossRef]
23 Weakley A. T.; Miller A. L.; Griffiths P. R.; Bayman S. J. Quantifying Silica in Filter-Deposited Mine Dusts Using Infrared Spectra and Partial Least Squares Regression. *Anal. Bioanal. Chem*., 2014, **406**, 4715-4724. [CrossRef]
24 Hassan A. F.; Abdelghny A. M.; Elhadidy H.; Youssef A. M. Synthesis and Characterization of High Surface Area Nanosilica from Rice Husk Ash by Surfactant-Free Sol–Gel Method. *J. Sol-Gel Sci. Technol.*, 2014, **69**, 465-472. [CrossRef]
25 Wanyika H.; Gachanja A. Instrumental Characterization of Montmorillonite Clays by X-Ray Fluorescence Spectroscopy, Fourier Transform Infrared Spectroscopy, X-Ray Diffraction and Uv/Visible Spectrophotometry. *J. Agric., Sci. Technol.*, 2016, **17**, 224-239. [Link]
26 Girsova M. A.; Golovina G. F.; Drozdova I. A.; Polyakova I. G.; Antropova T. V. Infrared Studies and Spectral Properties of Photochromic High Silica Glasses. *Opt. Appl*., 2014, **44**, 337-344. [CrossRef]
27 Hu S.; Hsieh Y. L. Preparation of Activated Carbon and Silica Particles from Rice Straw. *ACS Sustain. Chem. Eng*., 2014, **2**, 726-734. [CrossRef]
28 Ramasamy V.; Rajkumar P.; Ponnusamy V. Depth Wise Analysis of Recently Excavated Vellar River Sediments through FTIR and XRD Studies. *Indian J. Phys.*, 2009, **83**, 1295-1308. [CrossRef]
29 Mourhly A.; Khachani M.; Hamidi A. E.; Kacimi M.; Halim M.; Arsalane S. The Synthesis and Characterization of Low-cost Mesoporous Silica SiO_2 from Local Pumice Rock. *Nanomater. Nanotechnol.*, 2015, **5**, 1-7. [CrossRef]
30 Kaviyarasu, K.; Manikandan, E.; Kennedy, J.; Jayachandran, M.; Maaza, M. Rice Husks as a Sustainable Source of High Quality Nanostructured Silica for High Performance Li-Ion Battery Requital by Sol-Gel Method – A Review. *Adv. Mater. Lett.*, 2016, **7**, 684-696. [CrossRef]
31 Boza A. F.; Kupfer V. L.; Oliveira A. R.; Radovanovic E.; Rinaldi A. W.; Meneguin J. G.; Domingues N. L. C.; Moisés M. P.; Favaro S. L. Synthesis of α-aminophosphonates using a Mesoporous Silica Catalyst Produced from Sugarcane Bagasse Ash. *RSC Adv.,* 2016, **6**, 23981-23986. [CrossRef]
32 Orel B.; Jese R.; Stangar U. L.; Grdadolnik J.; Puchberger M. Infrared Attenuated Total Reflection Spectroscopy Studies of Aprotic Condensation of $(EtO)_3Si$-R-$Si(OEt)_3$ and R-$Si(OEt)_3$ Systems with Carboxylic Acids. *J. Non-Cryst.*, 2005, **351**, 530–549. [CrossRef]
33 Jagadesh P.; Ramachandramurthy A.; Murugesan R.; Sarayu K. Micro-analytical Studies on Sugar Cane Bagasse Ash. *Sadhana,* 2015, **40**, 1629-1638. [CrossRef]
34 Batra V. S.; Urbonaite S.; Svensson G. Characterization of Unburned Carbon in Bagasse Fly Ash. *Fuel*, 2008, **87**, 2972-2976. [CrossRef]
35 Agredo J. T.; Gutiérrez R. M.; Giraldo C. E. E.; Salcedo L. O. G. Characterization of Sugarcane Bagasse Ash as Supplementary Material for Portland Cement. *Ing. Investig*., 2014, **34**, 5-10. [Link]
36 Mueller R.; Kammler H. K.; Wegner K.; Pratsinis S. E. OH surface Density of SiO_2 and TiO_2 by Thermogravimetric Analysis. *Langmuir*, 2003, **19**, 160-165. [CrossRef]
37 Prasad T.; Halder S.; Dhar S. Process Parameter Effects on Particle Size Reduction of Sol-Gel Synthesized Silica Nanoparticles. *Mater. Today: Proceed.*, 2020, **22**, 1669–1675. [CrossRef]
38 Beganskienė A.; Sirutkaitis V.; Kurtinaitienė M.; Juškėnas R.; Kareiva A. FTIR, TEM and NMR Iinvestigations of Stöber Silica Nanoparticles. *Mater. Sci. (Medžiagotyra*), 2004, **10**, 287-290. [Link]
39 Mcdonald R. S. Surface Functionality of Amorphous Silica by Infrared Spectroscopy. *J. Phys. Chem.*, 1958, **62**, 1168-1178. [CrossRef]
40 Laufer S. Quantitative Determination of Surface Groups in Silica: IR-Analysis of Isolated Silanol Groups in Pyrogenic Silica. *J. Mol. Struct.*, 1980, **60**, 409-414. [CrossRef]
41 Rovani S.; Santos J. J.; Corio P.; Fungaro D. A. Highly Pure Silica Nanoparticles with High Adsorption Capacity Obtained from Sugarcane Waste Ash. *ACS Omega*, **2018**, **3**, 2618–2627. [CrossRef]